Journal of Neurochemistry
Lippincott Williams & Wilkins, Inc., Philadelphia

The Neuronal Microtubule-Associated Protein Tau Is a Substrate for Caspase-3 and an Effector of Apoptosis

*Luisa Fasulo, *Gabriele Ugolini, *Michela Visintin, *Andrew Bradbury, †Claudio Brancolini, *Vittorio Verzillo, *‡Michal Novak, and *Antonino Cattaneo

**Neuroscience Programme and INFM Unit, International School for Advanced Studies; †Laboratorio Nazionale Consorzio Interuniversitario Biotecnologie, Trieste, Italy; and ‡Institute of Neuroimmunology, Slovak Academy of Sciences, Dubravska, Bratislava, Slovakia*

Abstract: We have identified a class of tau fragments inducing apoptosis in different cellular contexts, including a human teratocarcinoma-derived cell line (NT2 cells) representing committed human neuronal precursors. We have found a transition point inside the tau molecule beyond which the fragments lose their ability to induce apoptosis. This transition point is located around one of the putative caspase-3 cleavage sites. This is the only site that can be effectively used by caspase-3 in vitro, releasing the C-terminal 19 amino acids of tau. These results establish tau as a substrate for an apoptotic protease that turns tau itself into an effector of apoptosis. Accordingly, tau may be involved in a self-propagating process like what has been predicted for the pathogenesis of different neurodegenerative disorders. **Key Words:** Microtubule—Tau—Apoptosis—Caspase-3.
J. Neurochem. **75,** 624–633 (2000).

Proteolysis of cellular proteins is one of the critical mechanisms of apoptosis (Salvesen and Dixit, 1997). Although many protein substrates for apoptosis-activated proteases have been identified, their functional significance is poorly understood. Some of these substrates are cytoskeletal proteins, for example, actin, fodrin, gelsolin, and GAS2 (Brancolini et al., 1995; Martin et al., 1995; Kayalar et al., 1996; Kothakota et al., 1997; Mashima et al., 1997; Geng et al., 1998; Janicke et al., 1998). The cleavage products of some of these substrates are effectors of apoptosis themselves, contributing to the biochemical and morphological changes that ultimately lead to cell death (Brancolini et al., 1995; Kothakota et al., 1997; Geng et al., 1998).

Inappropriate apoptosis in neurons accompanies many pathological changes in neurodegenerative disorders, such as Huntington's disease (Portera-Cailliau et al., 1995; Ona et al., 1999) and Alzheimer's disease (AD) (Anderson et al., 1996; Ugolini et al., 1997).

A growing body of evidence shows that the microtubule-associated protein tau (Mandelkow and Mandelkow, 1998; Spillantini and Goedert, 1998) is abnormally cleaved in AD and other tauopathies (Novak et al., 1991, 1993; Goedert et al., 1992; Johnson et al., 1997). The presence of cleaved tau in AD neurons is associated with expression of markers for neuronal death (Ugolini et al., 1997).

In a culture model of neuronal apoptosis, the production of tau fragments was shown to be an early and initially reversible event, with caspase-3 and calpain identified as proteases contributing to tau cleavage (Canu et al., 1998). A tau fragment including the microtubule-binding domains and both proline-rich regions was found to induce apoptosis when expressed in COS cells (Fasulo et al., 1998). In this article, we identify a class of fragments of human tau that display apoptotic capacity when expressed in different cells. Moreover, we find a transition point beyond which the fragments lose their ability to induce apoptosis. This transition point is located around one of the three putative caspase-3 cleavage sites that can be predicted in tau on the basis of sequence analysis. Only this site, in the C-terminal portion of the molecule, can be effectively used by caspase-3 in vitro. These findings establish tau as a substrate for an apoptotic protease that turns the remaining part of tau into an effector of apoptosis.

According to the present results, tau may be involved in a positive-feedback intracellular loop, an example of self-propagating process that has been predicted to underlie the pathogenesis of different neurodegenerative disorders (Yuan and Yankner, 1999).

Received October 20, 1999; revised manuscript received February 22, 2000; accepted March 23, 2000.

Address correspondence and reprint requests to Dr. A. Cattaneo at Neuroscience Programme, International School for Advanced Studies, Via Beirut 2/4, 34014 Trieste, Italy. E-mail: cattaneo@sissa.it

Drs. L. Fasulo, G. Ugolini, and M. Visintin contributed equally to this work.

Abbreviations used: AD, Alzheimer's disease; ISEL, in situ fragment end labeling; PARP, poly(ADP-ribose) polymerase; SDS-PAGE, sodium dodecyl sulfate–polyacrylamide gel electrophoresis.

MATERIALS AND METHODS

Expression plasmids

The expression vector pSG5 used for all the constructs and the plasmids dGAEpSG5, tau40pSG5, and tau151–391pSG5, directing the expression of the corresponding fragments of tau, were previously described (Fasulo et al., 1996, 1998). The numbering of tau fragments is according to the longest human tau isoform, tau40. Plasmids encoding tau fragments were generated by PCR using tau40pSG5 as a template. PCR primers contained *Eco*RI (5′) and *Bam*HI (3′) sites for insertion into *Eco*RI–*Bam*HI-cut pSG5.

The 5′ primer for tau151–402, tau151–412, tau151–422, tau151–432, tau151–441, tau151–274, tau151–336, and tau151–368 was 5′GCCCGAATTCATGATCGCCACACCGCGGGGAGCA3′. The 3′ primers were 5′TTACAGGATCCTCAGTCCCCAGACACCACTGGCGACTTGT3′, 5′TTACAGGATCCTCAGGAGACATTGCTGAGATGCCG3′, 5′TTACAGGATCCTCACGAGTCTACCATGTCGATGCT3′, 5′TTACAGGATCCTCACACCTCGTCAGCTAGCGTGGC3′, 5′TTACAGGATCCTCACAAACCCTGCTTGGCCAGGGA3′, 5′TTACAGGATCCTCACTTCCCGCCTCCCGGCTGGTG3′, 5′TTACAGGATCCTCACTGGCCACCTCCTGGTTTATG3′, and 5′TTACAGGATCCTCAATTTCCTCCGCCAGGGACGTG3′, respectively.

Constructs encoding for tau-head, P2dGAE, and Nt-dGAE were made using the following 5′ primers: 5′GCCCGAATTCATGGCTGAGCCCCGCCAGGAG3′ for tau-head and Nt-dGAE and 5′GCCCGAATTCATGAGCAGCCCCGGCTCCCCAGGC3′ for P2dGAE. The 3′ primers were 5′TTACAGGATCCTCAATTATCCTTTGAGCCACACTT3′ for tau-head and 5′TTACAGGATCCTCACTCCGCCCCGTGGTCTGTCTT3′ for P2 dGAE and Nt-dGAE.

Constructs encoding tau fragments tau1–422, tau22–441, and tau22–422 were made using the following 5′ primers: 5′GCCCGAATTCATGGCTGAGCCCCGCCAGGAG3′ for tau1–422 and 5′GCCCGAATTCATGGACAGGAAAGATCAGGGGGGC3′ for tau22–441 and tau22–422).

The 3′ primers were 5′TTACAGGATCCTCACGAGTCTACCATGTCGATGCT3′ for tau1–422 and tau22–422 and 5′TTACAGGATCCTCACAAACCCTGCTTGGCCAGGGA3′ for tau22–441.

Constructs encoding tau25* and tau421* were made using the following primers: 5′TTACAGGATCCTCACAAACCCTGCTTGGCCAGGGA3′ and 5′GCCCGAATTCATGGCTGAGCCCCGCCAGGAGTTCGAAGG3′ for tau ends, 5′GCCAGGAGTTCGAAGTGATGGAAGATCACGCTGGGACGTACGGGTTGGGCGATCGGAAAGCTCAGGGGGG3′ for caspase-3 site I, and 5′CCTCGTCAGCTAGCGTGGCCAGCTGGGGCGAGGCTACCATGTC3′ for caspase-3 site III.

PCR was carried out with Vent DNA polymerase in a PTC100 thermal cycler (MJ Research) for 30 cycles as follows: 94°C for 1 min, 60 or 65°C for 1 min, and 72°C for 1 min for 30 cycles, followed by 5 min at 72°C.

All amplified inserts were sequenced by the deoxynucleotide procedure of Sanger et al. (1977).

Cell culture, transfection, and analysis

COS cells were cultured and transiently transfected by the DEAE-dextran method as described elsewhere (Fasulo et al., 1996). Murine 3T3 fibroblasts, human NT2 teratocarcinoma cells, and human SH-SY5Y neuroblastoma cells were cultured in Dulbecco's modified Eagle's medium with 10% fetal calf serum (with high glucose, for NT2 cells), and transfected by the calcium phosphate method. Cells were analyzed 48 or 72 h after the transfection, respectively, for immunofluorescence and immunoblotting.

MN7.51 hybridoma supernatant, which recognizes all isoforms of human tau (Novak et al., 1991), was used at 1:20 dilution for both immunofluorescence and immunoblotting. Polyclonal antibody 304 (the generous gift of M. Goedert) was used at 1:1,000 dilution to detect tau-head (tau1–150). TRITC (tetramethylrhodamine isothiocyanate)-conjugated rabbit anti-mouse (1:200 dilution; Vector) or biotinylated anti-rabbit (1:500; Vector) and avidin rhodamine (1:1,000; Vector) were used for immunofluorescence. Peroxidase-conjugated goat anti-mouse and anti-rabbit secondary antibodies (DAKO) were used for immunoblotting at 1:1,000 dilution.

Apoptotic cells were identified in situ with the in situ fragment end labeling (ISEL) procedure for DNA fragmentation using the ApopTag direct in situ apoptosis detection kit (ONCOR), following the manufacturer's instructions (the procedure labels apoptotic nuclei with fluorescein). For double labeling, cells were fixed in 1% paraformaldehyde for 10 min on ice and then permeabilized with 70% ethanol (at −20°C) for 10 min. ApopTag staining for detection of DNA fragmentation was performed first, followed by indirect immunofluorescence (Fasulo et al., 1998). Coverslips were mounted in Vectashield mounting medium (Vector). Apoptotic transfected cells were visualized using a multiple wavelength filter (Zeiss Filter Set 25) and counted 48 h (72 h in the case of NT2 cells) after transfection (Fasulo et al., 1998). At least 500 transfected cells were examined for each construct. The average percentage of COS cells undergoing apoptosis, on expression of each tau construct, was calculated from at least three independent transfection experiments.

For western blotting, cells were collected 72 h after transfection, washed in phosphate-buffered saline, extracted with ice-cold microtubule-depolymerizing lysis buffer [50 m*M* Tris (pH 7.4), 2 m*M* $CaCl_2$, 1% NP-40, and a cocktail of protease inhibitors] for 20 min at 4°C, scraped off, and centrifuged 5 min at 12,000 rpm. Cell extracts were analyzed by sodium dodecyl sulfate–polyacrylamide gel electrophoresis (SDS-PAGE; 10% acrylamide), immunoblotted, and developed by the ECL method, according to the manufacturer's instructions (Amersham, Arlington Heights, IL, U.S.A.), or by incubating the blot for 2–10 min (at room temperature) with 0.05% 3,3′-diaminobenzidine (Sigma Chemical Co.) and 0.01% H_2O_2 in PBS.

In vitro translation and cleavage of tau with caspase-3

Recombinant human caspase-3 harboring a C-terminal hexahistidine tag was expressed in *Escherichia coli* and purified on a Ni^{2+} affinity resin, as described elsewhere (Canu et al., 1998). pSG5-based plasmids encoding for tau40, tau25* (D25A), and tau421* (D421A) were in vitro transcribed and translated with the transcription- and translation-coupled reticulocyte lysate system (Promega, Madison, WI, U.S.A.). Two microliters of translated reticulocyte lysate was incubated for 30 min at 37°C with purified caspase-3 in 10 μl of caspase-3 buffer containing protease inhibitors (Brancolini et al., 1997) in the presence or the absence of 200 n*M* *N*-acetyl-DEVD-aldehyde. Reactions were terminated by adding 1 volume of SDS-PAGE sample buffer and boiling for 3 min, before electrophoresis on SDS-PAGE.

RESULTS

A set of fragments of tau inducing apoptosis

Tau proteins are the main constituents of the paired helical filaments found in AD neurons (Wischik et al., 1988). All six full-length tau isoforms (Goedert et al., 1992) as well as shorter fragments (Novak et al., 1993) are present in paired helical filaments. In an attempt to investigate the impact of tau fragments on cell physiology, we initially focused our attention on the so-called 12-kDa tau fragments that encompass the microtubule-binding repeat regions. These fragments are unable to bind to microtubules but do not affect either cell morphology or viability (Fasulo et al., 1996). In a previous study, we showed that N-terminal extension of the 12-kDa fragment, including the two proline-rich regions (fragment tau151–391), induces apoptosis in COS cells (Fasulo et al., 1998).

To map systematically the apoptotic properties of tau, a set of fragments designed around tau151–391 and based on the longest tau isoform found in human brain (tau40) was engineered and expressed in cells.

Figure 1a shows a first set of constructs, starting at residue 151 (start of proline-rich region 1) and terminating at residues 391, 402, 412, 422, 432, and 441 (the natural end of tau protein). Plasmids directing the expression of these fragments were transiently transfected in COS cells, and the expression of the corresponding proteins was verified by western blotting (Fig. 1b), confirming that the fragments were expressed at comparable levels and displayed the predicted molecular weight.

Transfected cells were immunostained 48 h after transfection with the anti-tau monoclonal antibody MN7.51 (Fig. 1c–h). MN7.51 recognizes an epitope in the repeats region, contained in all constructs of this set. Cells expressing fragments tau40 (Fig. 1c), dGAE (Fig. 1d), and tau151–391 (Fig. 1e and f), tau151–422 (Fig. 1g), and tau 151–441 (Fig. 1h) were analyzed by double labeling with MN 7.51 (red) and with the ISEL procedure for DNA fragmentation (green), which reveals cell death. Tau fragments display a broad distribution throughout the cytosol with the fixation conditions used here, which do not allow visualization of the pool of microtubule-associated tau (when present), decorating the microtubule network.

Association with microtubules of ectopically overexpressed tau can be visualized when cell permeabilization is performed before fixation in microtubule-stabilizing conditions (Fasulo et al., 1996). In a previous study we have shown that the dGAE fragment of tau does not associate with microtubules (Fasulo et al., 1996).

The transfected cells expressing fragments of tau40 and showing DNA fragmentation were visualized using a multiple wavelength filter (Zeiss Filter Set 25), and the percentage of apoptotic cells of the total number of transfected cells was determined (Fig. 1i). The lowest percentage of DNA fragmentation was found in cells expressing the dGAE fragment, and for this reason this fragment was used as a negative control in all experiments. The level of apoptosis induced by the dGAE fragment corresponds to the background levels induced by negative controls in similar experimental conditions (Yamatsuji et al., 1996). The background incidence of apoptosis (corresponding to transfection-induced nonspecific cell damage) was negligible in our experimental condition. In contrast, the expression of fragments encompassing the proline-rich regions and terminating anywhere between residues 391 and 422 induced morphological changes typical of apoptosis (rounded shape, nuclear condensation, and membrane blebbing) as well as DNA fragmentation in a large number of cells (Fig. 1e–g). It is interesting that a further C-terminal extension of the fragments, to include the natural end of the protein, resulted in the complete loss of the apoptotic properties (Fig. 1i). In conclusion, all fragments terminating between amino acids 391 and 422 display the maximal ability to kill cells (40–45% of transfected cells being apoptotic, about a threefold increase in comparison with the dGAE negative control), with a sharp transition observed on further extension into the 19 C-terminal residues. No significant difference in the time of onset of the apoptotic effect was observed among the different tau deletion mutants.

The full-length tau40 protein induces a slightly higher level of apoptosis than the dGAE control fragment. This is most likely due to intracellular proteolysis of the molecule, as confirmed by western blot analysis (Fig. 1b), with the generation of apoptotic fragments. This may also be the case for the deletion mutants tau 151–432 and tau 151–441, which, like tau40, also display a modest apoptotic activity with respect to dGAE fragments, from which no apoptotic fragments can be generated. Alternatively, the slightly higher levels of apoptosis induced by full-length tau could also be ascribed to its microtubule-stabilizing capacity, as shown for Taxol-induced apoptosis in HL60 cells (Ibrado et al., 1996).

To characterize further the cell death process induced by the expression of these tau fragments, proteolytic cleavage of poly(ADP-ribose) polymerase (PARP) (Tewari et al., 1995) was assessed by immunoblot and demonstrated the appearance of the 85-kDa PARP band, diagnostic of apoptosis (data not shown). In cells coexpressing the fragment tau151–391 and the Bcl-2 anti-apoptotic protein, the processing of PARP to the 85-kDa band was significantly reduced (data not shown).

Fragment tau151–391 induces apoptosis in NT2 cells

Fragment tau151–391 was also expressed in mouse 3T3 fibroblasts, as well as in SH-SY5Y neuroblastoma and NT-2 teratocarcinoma cells, both human cell lines of neuronal origin. SH-SY5Y and NT-2 cells showed a similar behavior, and results are reported for NT2 cells in Fig. 2. The red fluorescence signal seen with the anti-tau MN 7.51 antibody is due to the transfected tau fragments because undifferentiated NT-2 cells do not express endogenous tau, as shown in Fig. 2d (lane A). A compar-

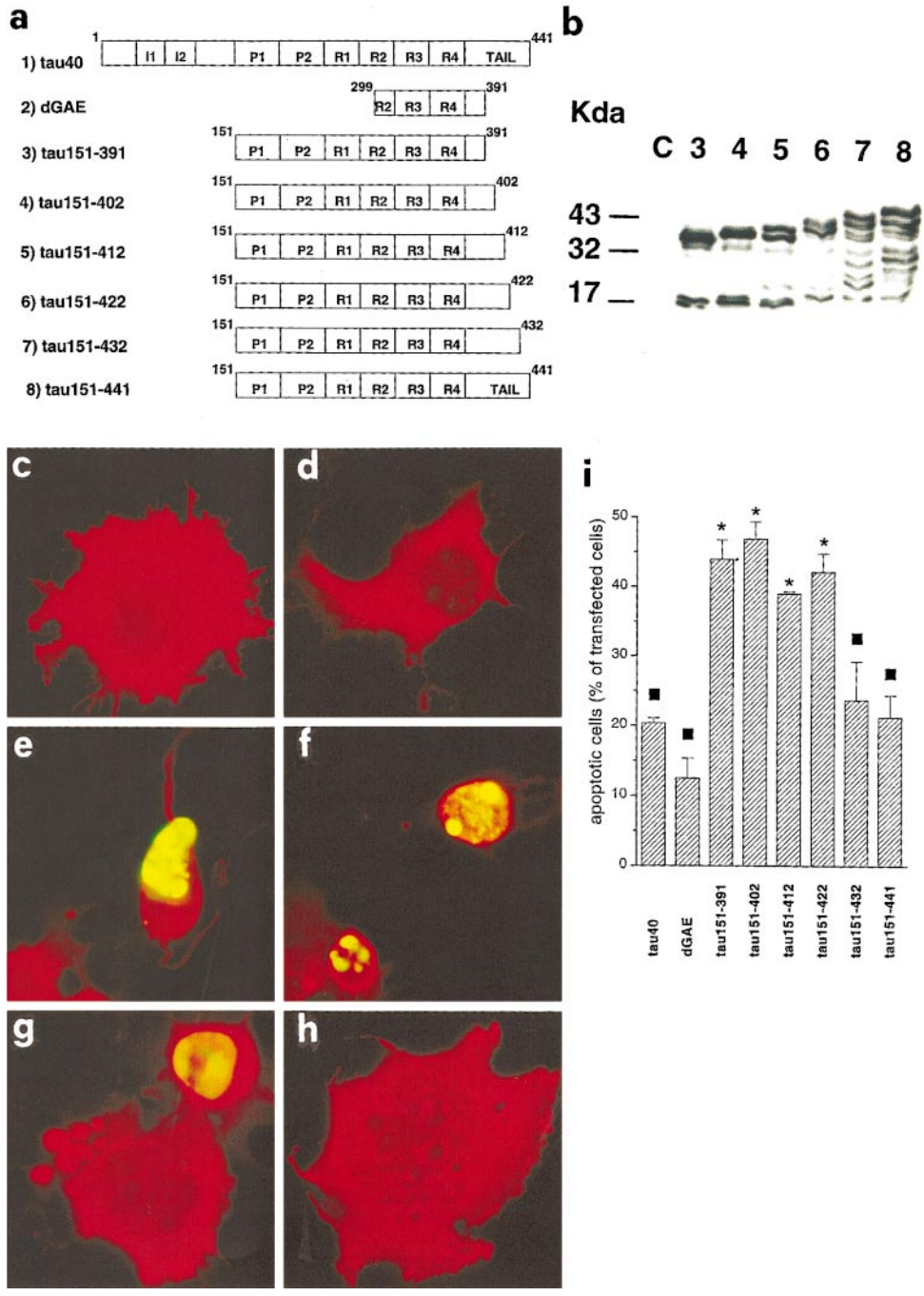

FIG. 1. A set of fragments of tau inducing apoptosis. **a:** Schematic representation of tau fragments. In this and in subsequent figures, the numbering of amino acids corresponds to that of the longest human brain tau isoform (tau40): 1, full-length tau40, where I1 and I2 are N-terminal inserts, P1 and P2 are proline-rich domains, and R1–R4 are microtubule-binding repeats; 2, dGAE, one of the AD paired helical filament core fragments; 3, tau151–391; 4, tau151–402; 5, tau151–412; 6, tau151–422; 7, tau151–432; and 8, tau151–441. **b:** Western blot of tau fragments expressed in COS cells. C, control untransfected cells. Lane numbers correspond to constructs in (a). Lanes 3–8, double labeling of COS cells expressing tau fragments. COS cells were transiently transfected with the tau constructs described in (a). Cells were analyzed 48 h after transfection by double labeling with the anti-tau monoclonal antibody MN 7.51 (red fluorescence) and with the ISEL procedure for DNA fragmentation (green fluorescence): (**c**) tau40, (**d**) dGAE, (**e** and **f**) tau151–391, (**g**) tau 151–422, and (**h**) tau 151–441. **i:** Percentage of cells transfected with tau fragments undergoing apoptosis. Average ± SE (bars) values from at least three independent transfection experiments are reported. At least 500 transfected cells were scored for each construct. Asterisks and solid squares over the columns indicate the statistical significance with respect to dGAE and to tau151–391, respectively ($p < 0.001$, except for tau 151–432, with $p < 0.05$).

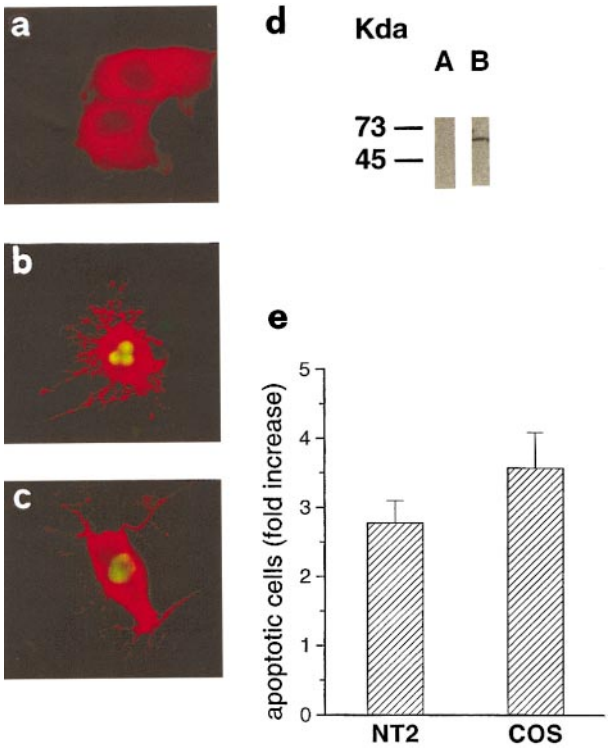

FIG. 2. Fragment tau151–391 induces apoptosis in human NT-2 cells. Human NT-2 cells were transiently transfected with the tau constructs (**a**) dGAE and (**b** and **c**) tau151–391. Cells were analyzed 72 h after transfection by double labeling with the anti-tau monoclonal antibody MN 7.51 (red fluorescence) and with the ISEL procedure for DNA fragmentation (green fluorescence). **d:** Undifferentiated NT-2 cells do not express endogenous tau, as revealed by a western blot comparison of cells transfected with tau40 (lane B) and untransfected NT-2 cells (lane A). **e:** The number of transfected cells undergoing apoptosis was evaluated 72 h after transfection. The ratio between the number of apoptotic cells observed with tau151–391 and that obtained with dGAE is expressed as fold increase of the number of apoptotic cells and is shown for both NT-2 and COS cell transfectants. Mean ± SE (bars) results from at least three independent transfection experiments for each cell line are reported. At least 500 transfected cells were scored for each construct.

ison of NT-2 cells expressing fragments dGAE (Fig. 2a) and tau151–391 (Fig. 2b and c) showed that the latter was able to induce apoptosis in these cells as well. The ratio between the number of apoptotic cells observed with tau151–391 and that obtained with dGAE (shown as fold increase of apoptotic cells) is comparable in NT-2 and COS cells (Fig. 2e). The fragment tau151–391 induces morphological changes not associated with DNA fragmentation in 3T3 fibroblasts and membrane blebbing and nuclear pyknosis in human SH-SY5Y neuroblastoma cells (data not shown).

Further mapping of apoptotic properties of tau fragments

A further mapping of the apoptotic properties of tau fragments showed that, unlike the C-terminal end, the N-terminal region did not appear to influence the apoptotic properties of tau fragments. Thus, fragment Nt-dGAE (tau1–391), encompassing the first 150 amino acids of tau (Fig. 3a), was as toxic as tau150–391 (Fig. 3b). Fragment tau-head, containing the N-terminal part alone (tau1–150; Fig. 3a), did not affect cell viability and was as harmless as the dGAE fragment (Fig. 3b).

In a subsequent series of experiments, the size of fragment tau151–391 was reduced at its N and C termini (Fig. 3c). N-terminal deletion of the first proline-rich region P1 and C-terminal shortening of at least one of the microtubule repeats reduce the apoptotic capacity of the fragment, to a level intermediate between that of tau151–391 and dGAE (Fig. 3d).

A transition point in the region immediately following residue 422 divides toxic from nontoxic fragments. The closeness of this transition point with a putative caspase-3 cleavage site, located at residue 421, suggested that the use of this site by caspase-3 in vivo could generate apoptotic fragments from the normal protein. Another potential caspase-3 recognition site starts at residue 22 of tau. To verify the impact on cell viability of tau fragments generated by the cleavage at either or both sites, the corresponding tau fragments tau1–422, tau22–441, and tau22–422 were expressed (Fig. 4a). The deletion of the 19 C-terminal residues of tau turned it into an effector of apoptosis, regardless of the presence of the initial 21 residues (compare fragments tau1–422 and tau22–422, Fig. 4b). In contrast, the expression of fragment tau22–441 yielded no substantial apoptotic effect (Fig. 4b).

Tau is substrate for caspase-3 in vitro

Tau contains three caspase-3 consensus recognition sequences, located at, respectively, residues 22–25 (site I), 338–341 (site II), and 418–421 (site III).

In previous work (Canu et al., 1998) we showed that, when in vitro translated tau was treated with caspase-3, the size of tau was reduced by ~5 kDa. This is consistent with cleavage at either or both sites I and III, whereas site II was unlikely to be used.

To elucidate which of the two sites is used by caspase-3, we generated tau mutants, in which sites I and III were individually abolished (Fig. 5a). In vitro translated tau40 and the two mutants tau25* and tau421* were treated with caspase-3 and analyzed by SDS-PAGE. The results showed that only site III was used by caspase-3, whereas sites I and II were not used (Fig. 5b). Indeed, the molecular weight shift observed on incubation with caspase-3 was only observed for tau40 (Fig. 5b, lanes 2 and 3) and tau25* (Fig. 5b, lanes 5 and 6), whereas tau421* was unaffected by the protease (Fig. 5b, lanes 8 and 9). The cleavage by caspase-3 was partially inhibited by the specific caspase-3 inhibitor *N*-acetyl-DEVD-aldehyde (Fig. 5b, lanes 4 and 7).

DISCUSSION

Neurodegeneration-associated gene products have been shown to be substrate for apoptotic proteases of the

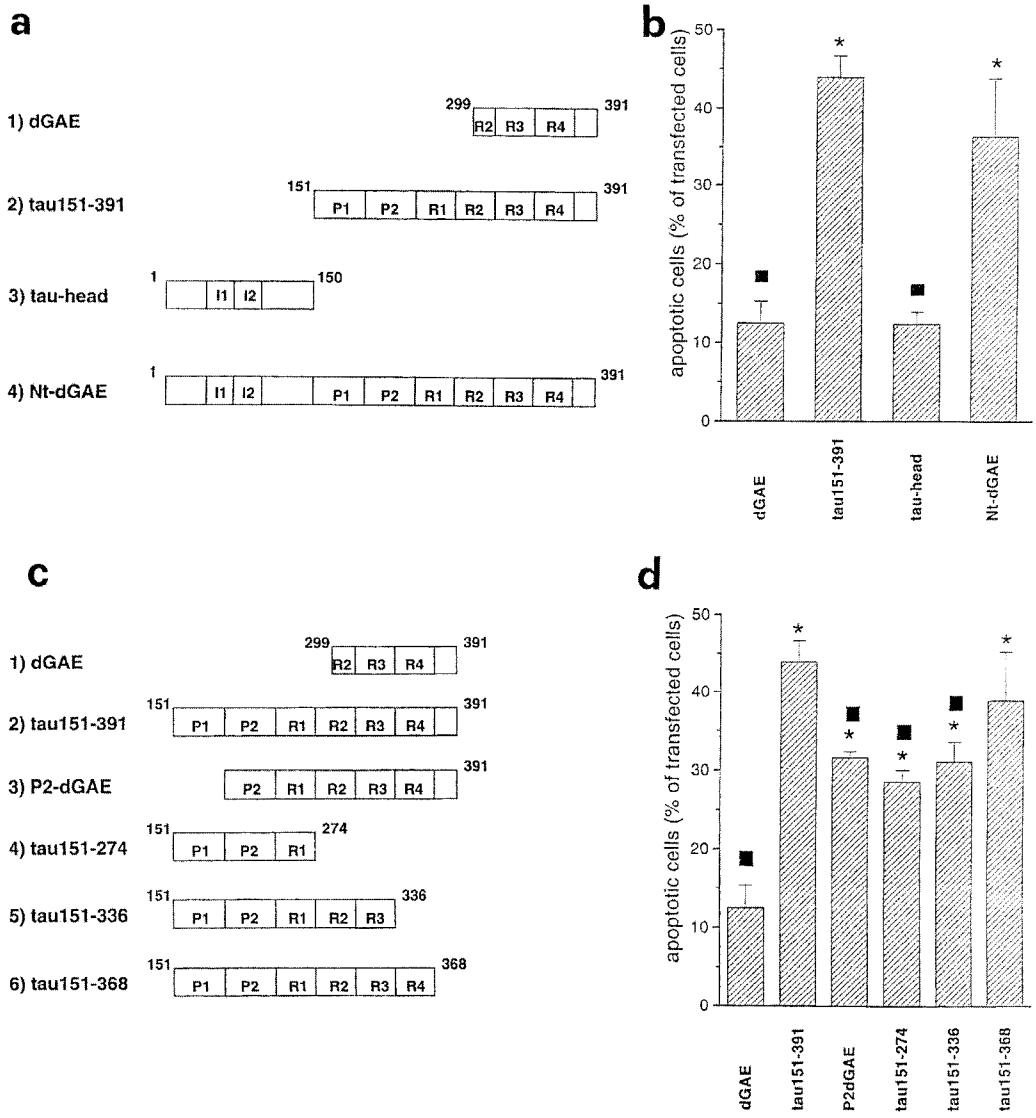

FIG. 3. Further mapping of the apoptotic properties of tau fragments. **a:** Schematic representation of tau fragments dGAE, tau151–391, tau-head, and Nt-dGAE. **b:** The N-terminal portion of tau does not influence the apoptotic properties of tau fragments as shown in apoptosis histograms. **c:** Schematic representation of tau fragments dGAE, tau151–391, P2-dGAE, tau 151–274, tau151–336, and tau151–368. **d:** Microtubule repeats and proline-rich regions contribute to the apoptotic properties of tau as shown in apoptosis histograms. The percentage of COS cells undergoing apoptosis, on transfection with the indicated tau constructs, was evaluated from at least three independent experiments. Results are mean ± SE (bars) values. At least 500 transfected cells were scored for each construct. Asterisks indicate the statistical significance with respect to dGAE ($p < 0.01$, at least, except for tau 151–368, with $p < 0.05$). Solid squares indicate the statistical significance with respect to tau151–391 ($p < 0.05$).

caspase family (Salvesen and Dixit, 1997). These include huntingtin and other polyglutamine expansion disease-associated proteins (Goldberg et al., 1996; Nasir et al., 1996; Wellington et al., 1998) as well as the AD-associated proteins presenilin-1, presenilin-2, and amyloid precursor protein (Kim et al., 1997; Loetscher et al., 1997; Barnes et al., 1998; Gervais et al., 1999; Van de Craen et al., 1999; Weidemann et al., 1999). On the other hand, many of the neurodegeneration-associated gene products induce a proapoptotic phenotype in cultured cells. These include polyglutamine expansion disease-associated proteins (Igarashi et al., 1998; Sanchez et al., 1999), mutant amyloid precursor protein (Yamatsuji et al., 1996) and presenilins (Mattson and Guo, 1997), and amyloidogenic Aβ-peptides (Yankner et al., 1989; Loo et al., 1993; LaFerla et al., 1995).

The microtubule-associated protein tau is the main component of the neurofibrillary lesions found in AD and in other neurodegenerative diseases, collectively known as tauopathies (Mandelkow and Mandelkow, 1998; Spillantini and Goedert, 1998). In a culture model of neuronal apoptosis, the production of tau fragments was shown to be an early and reversible event, with caspase-3 and calpain identified as proteases contributing

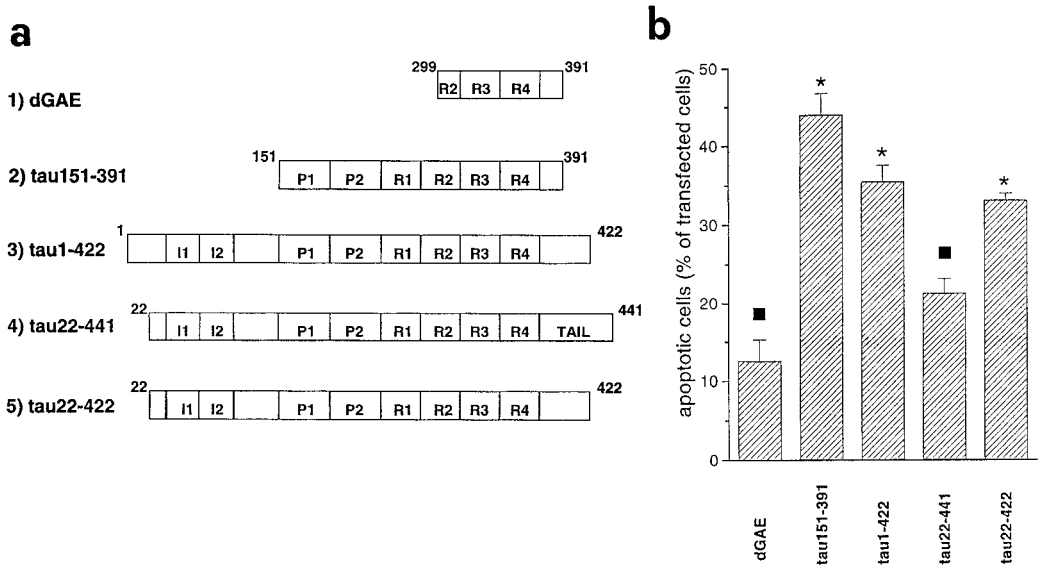

FIG. 4. Expression of tau fragments corresponding to cleavage at either or both the putative caspase-3 sites I and III. **a:** Schematic representation of tau fragments dGAE, tau151–391, tau1–422, tau22–441, and tau22–422. **b:** Quantification of the apoptosis induced by these constructs. The percentage of COS cells undergoing apoptosis, on transfection with the indicated tau constructs, was evaluated from at least three independent experiments. Results are mean ± SE (bars) values. At least 500 transfected cells were scored for each construct. Asterisks and solid squares over the columns indicate the statistical significance with respect to dGAE and to tau151–391, respectively ($p < 0.001$, except for tau151–432, with $p < 0.05$).

to tau cleavage in vivo (Canu et al., 1998). We have recently shown that the expression of a fragment of tau in COS cells induces cell death by apoptosis (Fasulo et al., 1998).

Thus, we postulate that tau may be part of a vicious circle, in which not only is it a substrate for proteases activated by subthreshold proapoptotic stimuli, but it also induces apoptosis by virtue of the fragments generated by those proteases. In this way, a positive-feedback intracellular loop involving tau would be generated, similar to the extracellular cycle that has been described for the neurotoxic fragments generated by caspase-3 cleavage of amyloid precursor protein (Gervais et al., 1999). This form of self-propagating degeneration has been proposed to apply to other proteins involved in neurodegenerative diseases (Yuan and Yankner, 1999).

The aim of the present work was to investigate the "apoptosis substrate and effector" hypothesis for tau. We identified a class of tau fragments displaying apoptotic capacity when expressed in different cells. The cell death process was defined as apoptosis according to the following criteria: (a) membrane blebbing and nuclear condensation and breakdown, (b) DNA fragmentation, (c) processing of PARP, and (d) protection by Bcl-2. Full apoptotic capacity (as displayed by fragments tau151–391 and tau151–422) corresponds to 45% of cells dying of the total number of COS cell transfectants. Deletion mapping experiments showed that the shortest fragment with full apoptotic capacity is tau151–368, which comprises the proline-rich regions P1 and P2 as well as the microtubule-binding domains R1 to R4. The longest fragment with full apoptotic capacity is tau1–422, which only lacks the 19 C-terminal residues.

We observed a transition point around residue 422, with C-terminal extension yielding a nontoxic protein, like full-length tau. This transition point overlaps with one of the three putative caspase-3 cleavage sites present in tau protein. We further showed that this site is the only one that can be effectively used by caspase-3 in vitro. This extends our previous work showing that tau could be cleaved by caspases in a culture model of neuronal apoptosis (Canu et al., 1998) and that one group of the toxic fragments of tau colocalizes with DNA fragmentation in AD neurons (Ugolini et al., 1997). Showing in vivo that apoptotic tau fragments are specifically generated in tau transfectants exposed to apoptotic stimuli will provide conclusive evidence in favor of the apoptotic substrate and effector hypothesis for tau. On the other hand, the possible involvement of caspase 3 also in the mechanism of apoptosis induced by tau fragments (besides its role in generating apoptotic tau fragments) represents a separate although related issue, the clarification of which will shed more light on the postulated positive feedback mechanism.

These results show that the absence of the 19 C-terminal residues of tau causes a dramatic change in the properties of the protein, turning it into an apoptotic effector. Various mechanisms can underlie this change: (a) Cleavage of the C-terminal peptide may cause a structural rearrangement of the remaining part of the molecule, possibly by preventing an intramolecular interaction; or (b) the C-terminal part of tau might be

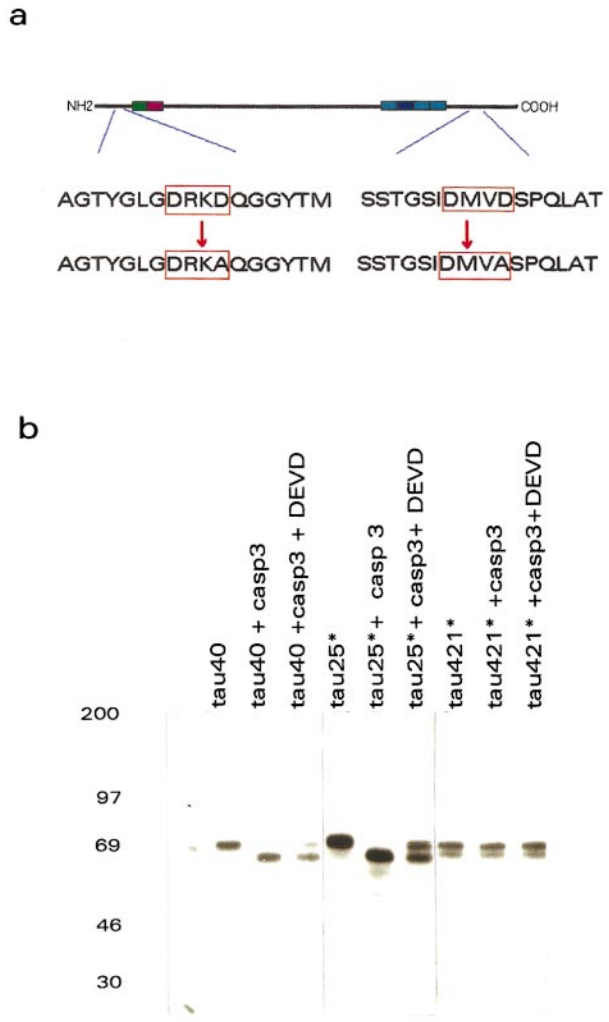

FIG. 5. In vitro cleavage of tau40 by caspase-3. **a:** Schematic representation of caspase-3 sites I and III on tau40. Caspase-3 consensus sequences I and III are shown (**upper row**), together with the mutations that were introduced to abolish them (**lower row**): tau25* (D25A) and tau421* (D421A). **b:** In vitro cleavage by caspase-3 of wild-type and mutant tau40. Tau proteins were in vitro translated in the presence of [^{35}S]methionine, incubated with recombinant caspase-3 in the presence or absence of 200 n*M N*-acetyl-DEVD-aldehyde (DEVD), electrophoresed on SDS-PAGE, and autoradiographed: lane 1, molecular weight marker; lanes 2–4, wild-type tau40 incubated with proteolysis buffer (lane 2), caspase-3 (lane 3), and caspase-3 with DEVD (lane 4); lanes 5–7, tau25* incubated with proteolysis buffer (lane 5), caspase-3 (lane 6), and caspase-3 with *N*-acetyl-DEVD-aldehyde (lane 7); and lanes 8–10, tau421* incubated with proteolysis buffer (lane 8), caspase-3 (lane 9), and caspase-3 with DEVD (lane 10).

involved in interactions with other cellular proteins, including tau itself. In this case, cleavage of this peptide would destroy these interactions. As a step toward a mechanistic understanding of the function of the C-terminal peptide, the solution structure of tau 423–441 was determined by NMR spectroscopy (Esposito et al., 2000). The peptide displays a well-defined right-handed α-helix structure, and the helical conformation is stabilized by a C-terminal capping motif, involving the glycine residue at the penultimate position. The structure exhibited by tau423–441 may play a role in the proteolysis of tau in the cell. Thus, an exposed frayed helix C-terminal end would not escape processing by cellular carboxypeptidases, leading to progressive unwinding of the helix. By contrast, a blocked helix should exhibit a greater resistance. Cleavage of tau at residue 421 by caspase-3 could make the protein more prone to further proteolysis, generating apoptotic fragments not containing the so-called site III for caspase 3.

It is noteworthy that isolated AD paired helical filaments, as well as AD neurons, contain a large number of fragments of tau (Novak et al., 1991, 1993; Goedert et al., 1992; Mercken et al., 1995; Bednarski and Lynch, 1996; Johnson et al., 1997). A large proportion of these fragments terminates at residue Glu^{391} (Novak et al., 1993; Ugolini et al., 1997). During C-terminal proteolysis, this residue might constitute an accumulation point that proteases are not able to overcome. Accumulation of fragments ending at Glu^{391} might be due to an intrinsic resistance to proteolysis of the upstream region, which has a predicted α-helical structure (Ruben et al., 1991), or to a concomitant pathological aggregation process, involving the microtubule-binding domains (Schweers et al., 1995). The relationship between tau aggregation and its apoptotic properties is presently unclear.

In conclusion, we have established a link between tau as a substrate of proteases activated in the course of apoptosis and the generation of tau fragments as effectors of apoptosis themselves, a feed-forward vicious circle that may affect cell viability starting from a subthreshold activation step. It is interesting that increased levels of caspase-3 have been recently found in dying neurons from human AD brains (Gervais et al., 1999).

Acknowledgment: We are grateful to M. Righi and G. Rossi for technical help. This work was supported by the INFM (Sez. B), Consiglio Nazionale delle Ricerche (PF Biotecnologie), TeleThon (grant E.1044 to A.C.), SIRS srl, and by grant 75195-54701 from Howard Hughes Medical Institute awarded to A.C. and M.N. L.F. acknowledges a fellowship from SIRS srl.

REFERENCES

Anderson A. J., Su J. H., and Cotman C. W. (1996) DNA damage and apoptosis in Alzheimer's disease: colocalization with c-Jun immunoreactivity, relationship to brain area, and effect of postmortem delay. *J. Neurosci.* **16,** 1710–1719.

Barnes N. Y., Li L., Yoshikawa K., Schwartz L. M., Oppenheim R. W., and Milligan C. E. (1998) Increased production of amyloid precursor protein provides a substrate for caspase-3 in dying motoneurons. *J. Neurosci.* **18,** 5869–5880.

Bednarski E. and Lynch G. (1996) Cytosolic proteolysis of τ by cathepsin D in hippocampus following suppression of cathepsins B and L. *J. Neurochem.* **67,** 1846–1855.

Brancolini C., Benedetti M., and Schneider C. (1995) Microfilament reorganization during apoptosis: the role of Gas2, a possible substrate for ICE-like proteases. *EMBO J.* **14,** 5179–5190.

Brancolini C., Lazarevich D., Rodriguez J., and Schneider C. (1997) Dismantling cell–cell contacts during apoptosis is coupled to

caspase-dependent proteolytic cleavage of β-catenin. *J. Cell Biol.* **139,** 759–771.

Canu N., Dus L., Barbato C., Ciotti M. T., Brancolini C., Rinaldi A. M., Novak M., Cattaneo A., Bradbury A., and Calissano P. (1998) Tau cleavage and dephosphorylation in cerebellar granule neurons undergoing apoptosis. *J. Neurosci.* **18,** 7061–7074.

Esposito G., Viglino P., Novak M., and Cattaneo A. (2000) The solution structure of a C-terminal peptide of human tau. *J. Pept. Sci.* (in press).

Fasulo L., Ovecka M., Kabat J., Bradbury A., Novak M., and Cattaneo A. (1996) Overexpression of Alzheimer's PHF core tau fragments: implications for the tau truncation hypothesis. *Alzheimers Res.* **2,** 195–200.

Fasulo L., Visintin M., Novak M., and Cattaneo A. (1998) Tau truncation in Alzheimer's disease: expression of a fragment encompassing PHF core tau induces apoptosis in COS cells. *Alzheimer's Rep.* **1,** 25–32.

Geng Y. J., Azuma T., Tang J. X., Hartwig J. H., Muszynski M., Wu Q., Libby P., and Kwiatkowski D. J. (1998) Caspase-3-induced gelsolin fragmentation contributes to actin cytoskeletal collapse, nucleolysis, and apoptosis of vascular smooth muscle cells exposed to proinflammatory cytokines. *Eur. J. Cell. Biol.* **77,** 294–302.

Gervais F. G., Xu D., Robertson G. S., Vaillancourt J. P., Zhu Y., Huang J., LeBlanc A., Smith D., Rigby M., Shearman M. S., Clarke E. E., Zheng H., Van Der Ploeg L. H., Ruffolo S. C., Thornberry N. A., Xanthoudakis S., Zamboni R. J., Roy S., and Nicholson D. W. (1999) Involvement of caspases in proteolytic cleavage of Alzheimer's amyloid-beta precursor protein and amyloidogenic Aβ peptide formation. *Cell* **97,** 395–406.

Goedert M., Spillantini M. G., Cairns N. J., and Crowther R. A. (1992) Tau proteins of Alzheimer paired helical filaments: abnormal phosphorylation of all six brain isoforms. *Neuron* **8,** 159–168.

Goldberg Y. P., Nicholson D. W., Rasper D. M., Kalchman M. A., Koide H. B., Graham R. K., Bromm M., Kazemi-Esfarjani P., Thornberry N. A., Vaillancourt J. P., and Hayden M. R. (1996) Cleavage of huntingtin by apopain, a proapoptotic cysteine protease, is modulated by the polyglutamine tract. *Nat. Genet.* **13,** 442–449.

Ibrado A. M., Huang Y., Fang G., and Bhalla K. (1996) Bcl-xL overexpression inhibits Taxol-induced Yama protease activity and apoptosis. *Cell Growth Differ.* **71,** 1087–1094.

Igarashi S., Koide R., Shimohata T., Yamada M., Hayashi Y., Takano H., Date H., Oyake M., Sato T., Sato A., Egawa S., Ikeuchi T., Tanaka H., Nakano R., Tanaka K., Hozumi I., Inuzuka T., Takahashi H., and Tsuji S. (1998) Suppression of aggregate formation and apoptosis by transglutaminase inhibitors in cells expressing truncated DRPLA protein with an expanded polyglutamine stretch. *Nat. Genet.* **18,** 111–117.

Janicke R. U., Ng P., Sprengart M. L., and Porter A. G. (1998) Caspase-3 is required for alpha-fodrin cleavage but dispensable for cleavage of other death substrates in apoptosis. *J. Biol. Chem.* **273,** 15540–15545.

Johnson G. V., Seubert P., Cox T. M., Motter R., Brown J. P., and Galasko D. (1997) The τ protein in human cerebrospinal fluid in Alzheimer's disease consists of proteolytically derived fragments. *J. Neurochem.* **68,** 430–433.

Kayalar C., Ord T., Testa M. P., Zhong L. T., and Bredesen D. E. (1996) Cleavage of actin by interleukin 1 beta-converting enzyme to reverse DNase I inhibition. *Proc. Natl. Acad. Sci. USA* **93,** 2234–2238.

Kim T. W., Pettingell W. H., Jung Y. K., Kovacs D. M., and Tanzi R. E. (1997) Alternative cleavage of Alzheimer-associated presenilins during apoptosis by a caspase-3 family protease. *Science* **277,** 373–376.

Kothakota S., Azuma T., Reinhard C., Klippel A., Tang J., Chu K., McGarry T. J., Kirschner M. W., Koths K., Kwiatkowski D. J., and Williams L. T. (1997) Caspase-3-generated fragment of gelsolin: effector of morphological change in apoptosis. *Science* **278,** 294–298.

LeFerla F. M., Tinkle B. T., Bieberich C. J., Haudenschild C. C., and Jay G. (1995) The Alzheimer's Aβ peptide induces neurodegeneration and apoptotic cell death in transgenic mice. *Nat. Genet.* **9,** 21–30.

Loetscher H., Deuschle U., Brockhaus M., Reinhardt D., Nelboeck P., Mous J., Grunberg J., Haass C., and Jacobsen H. (1997) Presenilins are processed by caspase-type proteases. *J. Biol. Chem.* **272,** 20655–20659.

Loo D. T., Copani A., Pike C. J., Whittemore E. R., Walencewicz A. J., and Cotman C. W. (1993) Apoptosis is induced by beta-amyloid in cultured central nervous system neurons. *Proc. Natl. Acad. Sci. USA* **90,** 7951–7955.

Mandelkow E. M. and Mandelkow E. (1998) Tau in Alzheimer's disease. *Trends Cell. Biol.* **8,** 425–427.

Martin S. J., O'Brien G. A., Nishioka W. K., McGahon A. J., Mahboubi A., Saido T. C., and Green D. R. (1995) Proteolysis of fodrin (non-erythroid spectrin) during apoptosis. *J. Biol. Chem.* **270,** 6425–6428.

Mashima T., Naito M., Noguchi K., Miller D. K., Nicholson D. W., and Tsuruo T. (1997) Actin cleavage by CPP-32/apopain during the development of apoptosis. *Oncogene* **14,** 1007–1012.

Mattson M. P. and Guo Q. (1997) Cell and molecular neurobiology of presenilins: a role for the endoplasmic reticulum in the pathogenesis of Alzheimer's disease? *J. Neurosci. Res.* **50,** 505–513.

Mercken M., Grynspan F., and Nixon R. A. (1995) Differential sensitivity to proteolysis by brain calpain of adult human tau, fetal human tau and PHF-tau. *FEBS Lett.* **368,** 10–14.

Nasir J., Goldberg Y. P., and Hayden M. R. (1996) Huntington disease: new insights into the relationship between CAG expansion and disease. *Hum. Mol. Genet.* **5,** 1431–1435.

Novak M., Jakes R., Edwards P. C., Milstein C., and Wischik C. M. (1991) Difference between the tau protein of Alzheimer paired helical filament core and normal tau revealed by epitope analysis of monoclonal antibodies 423 and 7.51. *Proc. Natl. Acad. Sci. USA* **88,** 5837–5841.

Novak M., Kabat J., and Wischik C. M. (1993) Molecular characterisation of the minimal protease resistant tau unit of the Alzheimer's disease paired helical filament. *EMBO J.* **12,** 365–370.

Ona V. O., Li M., Vonsattel J. P., Andrews L. J., Khan S. Q., Chung W. M., Frey A. S., Menon A. S., Li X. J., Stieg P. E., Yuan J., Penney J. B., Young A. B., Cha J. H., and Friedlander R. M. (1999) Inhibition of caspase-1 slows disease progression in a mouse model of Huntington's disease. *Nature* **399,** 263–267.

Portera-Cailliau C., Hedreen J. C., Price D. L., and Koliatsos V. E. (1995) Evidence for apoptotic cell death in Huntington disease and excitotoxic animal models. *J. Neurosci.* **15,** 3775–3787.

Ruben G. C., Iqbal K., Grundke-Iqbal I., Wisniewski H. M., Ciardelli T. L., and Johnson J. E. Jr. (1991) The microtubule-associated protein tau forms a triple stranded left-hand helical polymer. *J. Biol. Chem.* **266,** 22019–22027.

Salvesen G. S. and Dixit V. M. (1997) Caspases: intracellular signalling by proteolysis. *Cell* **91,** 443–446.

Sanchez I., Xu C. J., Juo P., Kakizaka A., Blenis J., and Yuan J. (1999) Caspase-8 is required for cell death induced by expanded polyglutamine repeats. *Neuron* **22,** 623–633.

Sanger F., Nicklen S., and Coulson A. R. (1977) DNA sequencing with chain-terminating inhibitors. *Proc. Natl. Acad. Sci. USA* **74,** 5463–5467.

Schweers O., Mandelkow E. M., Biernat J., and Mandelkow E. (1995) Oxidation of cysteine-322 in the repeat domain of microtubule-associated protein tau controls the in vitro assembly of paired helical filaments. *Proc. Natl. Acad. Sci. USA* **92,** 8463–8467.

Spillantini M. G. and Goedert M. (1998) Tau protein pathology in neurodegenerative diseases. *Trends Neurosci.* **21,** 428–433.

Tewari M., Quan L. T., O'Rourke K., Desnoyers S., Zeng Z., Beidler D. R., Poirier G. G., Salvesen G. S., and Dixit V. M. (1995) Yama/CPP32 beta, a mammalian homolog of CED-3, is a CrmA-inhibitable protease that cleaves the death substrate poly(ADP-ribose) polymerase. *Cell* **81,** 801–809.

Ugolini G., Cattaneo A., and Novak M. (1997) Co-localisation of truncated tau and DNA fragmentation in Alzheimer's disease neurones. *Neuroreport* **8,** 3709–3712.

Van de Craen M., De Jonghe C., Van den Brande I., Declercq W., Van Gassen G., Van Criekinge W., Vanderhoeven I., Fiers W., Van Broeckhoven C., Hendriks L., and Vandenabeele P. (1999) Identification of caspases that cleave presenilin-1 and presenilin-2. Five presenilin-1 (PS1) mutations do not alter the sensitivity of PS1 to caspases. *FEBS Lett.* **445,** 149–154.

Weidemann A., Paliga K., Durrwang U., Reinhard F. B., Schuckert O., Evin G., and Masters C. L. (1999) Proteolytic processing of the Alzheimer's disease amyloid precursor protein within its cytoplasmic domain by caspase-like proteases. *J. Biol. Chem.* **274,** 5823–5829.

Wellington C. L., Ellerby L. M., Hackam A. S., Margolis R. L., Trifiro M. A., Singaraja R., McCutcheon K., Salvesen G. S., Propp S. S., Bromm M., Rowland K. J., Zhang T., Rasper D., Roy S., Thornberry N., Pinsky L., Kakizuka A., Ross C. A., Nicholson D. W., Bredesen D. E., and Hayden M. R. (1998) Caspase cleavage of gene products associated with triplet expansion disorders generates truncated fragments containing the polyglutamine tract. *J. Biol. Chem.* **273,** 9158–9167.

Wischik C. M., Novak M., Thogersen H. C., Edwards P. C., Runswick M. J., Jakes R., Walker J. E., Milstein C., Roth M., and Klug A. (1988) Isolation of a fragment of tau derived from the core of the paired helical filament of Alzheimer disease. *Proc. Natl. Acad. Sci. USA* **85,** 4506–4510.

Yamatsuji T., Okamoto T., Takeda S., Murayama Y., Tanaka N., and Nishimoto I. (1996) Expression of V642 APP mutant causes cellular apoptosis as Alzheimer trait-linked phenotype. *EMBO J.* **15,** 498–509.

Yankner B. A., Dawes L. R., Fisher S., Villa-Komaroff L., Oster-Granite M. L., and Neve R. L. (1989) Neurotoxicity of a fragment of the amyloid precursor associated with Alzheimer's disease. *Science* **245,** 417–420.

Yuan J. and Yankner B. A. (1999) Caspase activity sows the seeds of neuronal death. *Nat. Cell. Biol.* **1,** E44–E45.